Heterogeneous Void Formation in 14 MeV Nickel-Ion-Irradiated 316 SS

R.L. Sindelar, G.L. Kulcinski and R.A. Dodd

November 1984

UWFDM-604

Presented at the First International Conference on Fusion Reactor Materials, Tokyo, Japan, 3-6 December 1984.

FUSION TECHNOLOGY INSTITUTE

UNIVERSITY OF WISCONSIN

MADISON WISCONSIN

Heterogeneous Void Formation in 14 MeV Nickel-Ion-Irradiated 316 SS

R.L. Sindelar, G.L. Kulcinski and R.A. Dodd

Fusion Technology Institute
University of Wisconsin
1500 Engineering Drive
Madison, WI 53706

http://fti.neep.wisc.edu

November 1984

UWFDM-604

Presented at the First International Conference on Fusion Reactor Materials, Tokyo, Japan, 3-6 December 1984.

HETEROGENEOUS VOID FORMATION IN 14 MeV NICKEL-ION-IRRADIATED 316 SS[†]

R.L. Sindelar, G.L. Kulcinski and R.A. Dodd

Fusion Technology Institute
1500 Johnson Drive
University of Wisconsin-Madison
Madison, Wisconsin 53706

December 1984

UWFDM-604

[†]Presented at the First International Conference on Fusion Reactor Materials, Tokyo, Japan, 3-6 December 1984.

HETEROGENEOUS VOID FORMATION IN 14 MeV NICKEL-ION-IRRADIATED 316 SS

R.L. Sindelar, G.L. Kulcinski and R.A. Dodd

Fusion Technology Institute
University of Wisconsin
Madison, WI 53706

ABSTRACT

The microstructure of type 316 austenitic stainless steel has been investigated following 14 MeV Ni-ion irradiation to 3.3 x 10^{16} ions/cm^2 (40 dpa peak damage) at temperatures from 450°C to 650°C. Specimens were prepared in cross section to allow analysis over the entire damage range, and the void parameters, dislocation structure, and precipitation response are reported. Heterogeneous void formation was observed in the absence of gas. The swelling curve from this study has been compared to that derived from helium preinjection work. It was found that helium shifts the peak swelling temperature upwards in excess of 100°C for similar damage rates. The precipitation response shows a marked change from small block/rod morphology at 450-550°C to Fe_2P thin lathe precipitates at 600-650°C. Void formation was detected only for the lower temperature range and was associated with the small block/rod precipitates.

Introduction

Ion irradiation studies are a useful tool to investigate the irradiation response of a material while closely controlling irradiation parameters such as temperature, dose rate, helium injection, etc. In addition, information relevant to basic models of microstructural evolution can be readily generated which may lead to a better understanding of the mechanisms of swelling resistance [1-4].

The present investigation deals with 14 MeV Ni-ion irradiations of 316 stainless steel. The use of high energy heavy ions and the cross section technique [5] allows data analysis in a damage region free from surface effects and any effects of the injected bombarding ion species [6]. This paper reports the microstructural response of type 316 austenitic stainless steel to a nickel-ion irradiation over the 450-650°C temperature range.

Experimental Procedure

Table 1 contains the elemental composition of the MFE heat of 316 SS used in this study. Samples of this material were mechanically polished with 0.3 μm alumina abrasive prior to being irradiated with 14 MeV Ni^{3+} ions at the University of Wisconsin Heavy-Ion Irradiation Facility. The samples were not electropolished before irradiation in order to preclude the introduction of hydrogen into the specimen, which has been shown to enhance cavity formation in nickel [5,7].

Figure 1 shows the displacement damage as a function of depth for 14 MeV Ni ions on a 316 stainless steel target. For comparison purposes, we have chosen a displacement efficiency factor of K = 0.8 in this study to calculate the displacement damage. However, the use of K = 0.3 is probably a more

appropriate measure of the residual displacement damage for neutrons or ions [6]. Nevertheless, the damage values in this paper will be derived from a K = 0.8 value to be consistent with the previous decade of ion bombardment studies.

Specimens were irradiated over a 450-650°C temperature range at a flux of 3×10^{11} ions/cm^2/s to a fluence of 3.3×10^{16} ions/cm^2. This corresponds to a peak displacement dose of 40 dpa at a depth of 2.3 μm from the specimen surface. Post-irradiation preparation for TEM analysis involved a cross section technique described in detail elsewhere [8]. This procedure allows the entire 3 micron damage region (see Fig. 1) to be analyzed for an irradiated sample. The microscopy analysis was performed using a JEOL TEMSCAN-200CX electron microscope.

Results

Voids were detected in the samples irradiated in the range 450-550°C. No voids were found, however, after irradiation at 600°C and 650°C to a peak dose of 40 dpa. Figure 2 contains the through-range transmission electron micrographs of 500°C samples irradiated to 3.3×10^{16} ions/cm^2 and 1.0×10^{17} ions/cm^2. From this figure it is evident that the formation of the voids is heterogeneous throughout the damage region, that is, voids formed only at some of the precipitate sites present in the matrix. This heterogeneous void density is also present in the 450°C and 550°C samples. Figure 3 contains high magnification TEM micrographs which reveal voids associated with precipitates over the entire temperature range of void detection. The voids are decorated by or are associated with precipitates. The void parameters obtained at the 1 μm depth (10 dpa) and 2.3 μm depth (40 dpa) are given in Table 2. The displacement rates at these depths were approximately 0.8×10^{-3} dpa/s and 3.6 x

10^{-3} dpa/s respectively (see Fig. 1). An error of 30-40% is assigned to the void and precipitate number densities to account mainly for the uncertainty in the foil thickness as well as the statistical counting uncertainty at the given depth.

Table 3 lists the dislocation structure obtained from the 1 μm depth (10 dpa) and the 2.3 μm depth (40 dpa) of the cross-sectioned specimens. The dislocation loops were predominantly faulted loops that increased in average loop diameter and decreased in loop density with increasing temperature for a common dose irradiation. Saturation in the network dislocation density at 2 x 10^{10} cm^{-2} was also noted between 550°C-650°C at these doses.

A key microstructural response of the 316 SS in the 600-650°C range was the formation of the Fe_2P phase, which has a needle-shaped appearance (see Fig. 4). Results from the 600°C sample show the Fe_2P precipitates have an average length of 54 nm with a density of 9.9 x 10^{14} cm^{-3} at the 1 μm depth (10 dpa) and an average length of 58 nm with a density of 1.2 x 10^{15} cm^{-3} at the damage peak (40 dpa) depth. At 650°C there was an increase in the average length with a corresponding decrease in number density of the precipitates at both depths compared to the 600°C results. The region at a 1 μm depth (650°C sample) contained phosphides of average length 92 nm with density 2.3 x 10^{14} cm^{-3}, while the average length and density showed a slight increase to 99 nm and 2.6 x 10^{14} cm^{-3}, respectively, at the 2.3 μm depth. These phosphides were extracted from the matrix on a plastic replica. EDS analysis yielded a chemical composition of 4Si-3P-2S-18Cr-61Fe-12Ni. In addition, a plated specimen was given a post-irradiation anneal at the prevailing irradiation temperature of 650°C for 24 hours. No phosphide needles were detected in the irradiated

region of this specimen after the anneal. This composition and annealing behavior is similar to Fe_2P detected in other ion-irradiation studies of 316 SS [9].

The precipitation response in the 450-550°C range was characterized by small block/rod precipitates. The average size was 9.2 nm with density 1.1×10^{15} cm^{-3} at the 1 μm (10 dpa) depth and 16 nm with density 6.5×10^{14} cm^{-3} at the 2.3 μm (40 dpa) depth for the 500°C sample. Most of the precipitates at the 1 μm depth formed in stringers and some precipitates at the damage peak were associated with voids. Diffraction information from some of the larger precipitates showed them to have an fcc structure with lattice parameter 1.1 nm. No particular habit relationship to the matrix was observed. In addition, x-ray spectra obtained using an HB 501 STEM with an EDS detector revealed a strong enrichment of nickel in these precipitates. These results suggest that this phase is the radiation-induced G phase, a nickel silicide [10].

At 550°C the average length of the precipitates was 35 nm with density 1.2×10^{15} cm^{-3} at 1 μm (10 dpa) and 36 nm with density 2.7×10^{14} cm^{-3} at the 2.3 μm depth (40 dpa). Quantitative information on precipitation at 450°C was difficult to measure and so is not reported.

Discussion

The void swelling results at 40 dpa in this study are plotted in Fig. 5 along with the void swelling data of Hudson [11]. In that study, 316 SS and 321 SS whose compositions are given in Table 1 were preinjected with helium to 10 appm and irradiated to 40 dpa at a rate of $1\text{-}3 \times 10^{-3}$ dpa/s with 46.5 MeV nickel ions. Data for the swelling curves plotted in Fig. 5 was taken from the peak damage region in each study (at ≈ 2 μm in this study, 4.5 μm in

Hudson study). The displacement rates were similar ($\approx 3 \times 10^3$ dpa/s) and damage gradient effects were precluded by data acquisition at a given depth, i.e. dose (in this case, 40 dpa). It may be argued that void data extracted in the damage peak is influenced by the injected ion species [6]. However results of a recent study show that void nucleation and growth was important at temperatures $\leq$ 500°C for an austenitic stainless steel alloy. Thus the absence of voids at 600 and 650°C in this present study cannot be ascribed to injected interstitial effects. In addition to the large difference in the amount of swelling, a "shift" in excess of 100°C between the peak swelling temperatures is noted for this common dose swelling plot. This "shift" is actually a suppression of void formation at 600 and 650°C in this present study. The lack of void formation is attributed to the absence of helium as a nucleating agent which acts to pressurize and thus stabilize subcritical cavities [12-14]. The large difference in the absolute value of swelling between the data is again attributed to the action of helium affecting the cavity growth rate through pressurization of the cavity [15]. The differences in the level of impurities between the two heats of 316 SS (Table 1) would not account for the large temperature "shift" in peak swelling [16]. In addition, Hudson found little difference in peak swelling temperatures for the 316 SS and 321 SS (Table 1) in his study.

Farrell and Packan [17] have also reported a helium-induced upward shift in the temperature dependence of swelling in the P7 alloy. This alloy is similar in composition to 316 SS but with a low level of carbon and minor metallic elements and a high level (1000 appm) of oxygen. They determined the peak swelling temperature for 4 MeV Ni ion-irradiated P7 to be approximately 670°C [17]. Our recent work with 14 MeV Ni ions [18] agrees with their

results as we found 7% swelling in P7 at 650°C for a dose of 40 dpa (E_d = 40 eV, K = 0.8). Our study attributed the large swelling in P7 to the high oxygen concentration which would effect the nucleation and growth of voids by lowering their surface energy. P7 is considered a "pure 316 SS" as it is low in carbon and other impurity elements nominally present in 316 SS (see Table 1). It is well known that impurities suppress the swelling response of Fe-Cr-Ni alloys [16]. Makin [19] has found, however, that there is no difference in the peak swelling temperatures between a 316 L (with 0.01 C, 0.04 Si), 316 M (0.06 C, 0.36 Si), and 316 H (0.2 C, 0.4 Si). Thus the difference in peak swelling temperatures between the 316 SS used in this study and the P7 alloy might be attributed to an oxygen-induced shift in the temperature dependence of swelling. A study whereby a controlled oxygen content is present in 316 SS would be needed to confirm this speculation.

Helium and/or reactive gases (e.g., O, H) are well recognized for their importance in void formation [12-14, 20-22]. The 316 SS used in this study, however, contained a nominal oxygen and hydrogen content. In addition, the heterogeneous nature of void nucleation would suggest a different mechanism for void stabilization. Several authors have suggested such a concept based on the biasing of void embryos against interstitial capture through means of solute enrichment at the void surface [23,24]. This segregation can cause the local lattice parameter near the void to increase and thereby reverse the interstitial bias of a small void [23].

It has been noted [25] that titanium-modified steels effectively getter reactive gases and thereby resist void formation under irradiation unless helium is present. In a titanium-modified steel irradiated with 4 MeV Ni ions at 625°C, Kenik and Lee [26] detected no voids after a dose of ~ 600 dpa.

Results of this present study suggest that their irradiation temperature may be too high to permit void nucleation in the absence of gases.

A difference in the precipitation response was noted in this study between the specimens irradiated at 450-550°C and those irradiated at 600-650°C. Whereas many of the precipitates detected after irradiation at 450-550°C and tentatively identified as G phase were small rod or block shaped, those at 600-650°C were predominantly an Fe_2P phase with a thin lathe morphology which has a needle-like appearance in a TEM specimen. Although this change in response coincides with the temperature above which voids are not detected, no correlation of these phenomena is apparent at the present time.

Conclusions

Microstructural observations were made on solution annealed type 316 stainless steel following 14 MeV Ni-ion irradiations to a peak dose of 40 dpa at temperatures from 450°C to 650°C. The following conclusions can be drawn:

1. This MFE heat of 316 SS was seen to exhibit a peak swelling temperature near 525°C following irradiation at 1-4 x 10^{-3} dpa/s to 40 dpa.
2. Heterogeneous void formation was detected in 316 SS irradiated at 450-550°C and the voids possessed a strong association with precipitates.
3. The precipitation response during irradiation showed a marked difference between the 450-550°C temperature range and the 600-650°C range. Nickel rich precipitates characteristic of G phase were found in the low temperature regime, whereas an Fe_2P phase formed at the higher temperatures.

Acknowledgements

The authors wish to thank Professor T.F. Kelly for his experimental assistance. Support for this work provided by the U.S. Department of Energy.

References

1. R.S. Nelson, et al., in Radiation-Induced Voids in Metals, Proceedings of the 1971 International Conference held at Albany, New York, June 1971, J.W. Corbett and L.C. Ianiello, Eds.

2. F.A. Garner and W.G. Wolfer, in Effects of Radiation on Materials: Eleventh Conference, ASTM STP 782, H.R. Brager and J.S. Perrin, Eds. (1982) 1073-1087.

3. J.F. Bates and W.G. Johnston, in Proceedings of the International Conference on Radiation Effects in Breeder Reactor Structural Materials, M.L. Bleiberg and J.W. Bennett, Eds. AIME (1977), 625-644.

4. J.O. Stiegler, J.M. Leitnaker and E.E. Bloom, in Physical Metallurgy of Reactor Fuel Elements, J.E. Harris and E.C. Sykes, Eds., The Metals Society (1975) 136.

5. J.B. Whitley, Ph.D. Thesis, University of Wisconsin, 1978.

6. B. Badger, et al., "Experimental Investigation of the Effect of Injected Interstitials on Void Nucleation", 12th Intern. Symp. on Effects of Radiation on Materials, Williamsburg, VA, 1984.

7. D.B. Bullen, Ph.D. Thesis, University of Wisconsin, 1984.

8. R.L. Sindelar, G.L. Kulcinski and R.A. Dodd, J. Nucl. Mater. 122 & 123 (1984) 246-251.

9. E.H. Lee, L.K. Mansur and A.F. Rowcliffe, J. Nucl. Mater. 122 & 123 (1984) 299-304.

10. W.J.S. Yang, H.R. Brager and F.A. Garner in Phase Stability During Irradiation, L.K. Mansur and D.I. Potter, Eds., (1980) 257-269.

11. J.S. Hudson, J. Nucl. Mater. 60 (1976) 89.

12. L.A. Parker and K.C. Russell, Scripta Met. 15 (1981) 643-647.

13. J.R. Townsend, J. Nucl. Mat. 108 & 109 (1982) 544-549.

14. L.K. Mansur and N.A. Goghlan, J. Nucl. Mat. 119 (1983) 1-25.

15. L.K. Mansur, Nucl. Tech. Vol. 40 (1978) 5.

16. See, for example "Radiation Effects in Breeder Reactor Structural Materials", M.L. Bleiberg and J.W. Bennett, Eds. AIME (1977).

17. K. Farrell and N.H. Packan, J. Nucl. Mater. 85 & 86 (1979) 683-687.

18. R.L. Sindelar, R.A. Dodd and G.L. Kulcinski, "A Comparison of Depth-Dependent Microstructures of Ion-Irradiated 316 Type Stainless Steels," 12th Intern. Symp. on Effects of Radiation on Materials, Williamsburg, VA, 1984 ASTM STP 870, F.A. Garner and J.S. Perrin, Eds.

19. M.J. Makin, et al., in Ref. 16 p. 660.

20. K. Farrell, Rad. Effects 53 (1980) 175-194.

21. L.D. Glowinski and C. Fiche, J. Nucl. Mater., 61 (1976) 22-28.

22. W.G. Wolfer, J. Nucl. Mater. 122 & 123 (1984) 367-378.

23. A. Si-Ahmed and W.G. Wolfer in Effects of Radiation on Materials: Eleventh Conference ASTM STP 782, H.R. Brager and J.S. Perrin, Eds. (1982).

24. W.G. Wolfer, L.K. Mansur and J.A. Sprague in Proceedings of the International Conference on Radiation Effects in Breeder Reactor Structural Materials, M.L. Bleiberg and J.W. Bennett, Eds. AIME (1977) 841.

25. P.J. Maziasz, J. Nucl. Mater. 122 & 123 (1984) 472-486.

26. E.A. Kenik and E.H. Lee in Phase Stability During Irradiation, L.K. Mansur and D.I. Potter, Eds. (1980) 493-503.

27. D.K. Brice, "Ion Implantation Range and Energy Deposition Codes COREL, RASE 4, and DAMG2," SAND77-0622, Sandia National Lab. (1977).

Table 1. Composition of the MFE Heat (#15893) 316 SS, the P7 Alloy, the Firth-Vickers 555 316 SS, and the En58B 321 SS in wt.%. The Oxygen and Nitrogen Contents were Determined by Inert-Gas Fusion Analysis.

MFE 316 SS

Cr	Ni	Mo	Mn	Si	C	P	S	Ti	O	N	Fe
17.4	12.6	2.2	1.81	0.65	0.05	0.030	0.020	< 0.001	0.005	0.046	Bal.

Firth Vickers 555 316 SS

Cr	Ni	Mo	Mn	Si	C	P	S	Ti	O	N	Fe
17.5	11.8	2.5	1.1	0.3	0.03					0.023	Bal.

En58B 321 SS

Cr	Ni	Mo	Mn	Si	C	P	S	Ti	O	N	Fe
18.1	9.57		1.76	0.42	0.05	0.025	0.03	0.33			Bal.

P7 Alloy

Cr	Ni	Mo	Mn	Si	C	P	S	Ti	O	N	Fe
17	16.7	2.5	0.03	0.1	0.005			0.01	0.03	0.004	Bal.

Table 2. Void Parameters for Nickel Ion Irradiated 316 SS.

Temperature (°C)	Dose (dpa)	Mean Void Diameter (nm)	Void Density (cm^{-3})	Swelling (%)
450	10*	7.5	4×10^{14}	0.02
	40**	12	5×10^{14}	0.04
500	10*	21	1.3×10^{14}	0.08
	40**	24	2.3×10^{14}	0.17
500	30[a]	25	0.91×10^{14}	0.07
	120[aa]	30	1.4×10^{14}	0.20
550	10*	20	1.5×10^{14}	0.05
	40**	25	2.1×10^{14}	0.18

* Taken at 1 micron from front surface, 0.8×10^{-3} dpa/s.

** Taken at 2.3 microns from front surface, 3.2×10^{-3} dpa/s.

[a] Taken at 1 micron from front surface, 1.4×10^{-3} dpa/s.

[aa] Taken at 2.3 micron from front surface, 5.5×10^{-3} dpa/s.

Table 3. Dislocation Structure for Ion-Irradiated 316 SS

Temperature (°C)	Dose (dpa)	Average Loop Diameter (nm)	Loop Density (cm^{-3})	Network Density (cm^{-2})
450	10*	30	2.8×10^{15}	---
	40**	32	3.0×10^{15}	---
500	10*	46	1.6×10^{15}	---
	40**	47	1.4×10^{15}	---
550	10*	42	1.3×10^{15}	1.0×10^{10}
	40**	34	2.0×10^{15}	2.1×10^{10}
600	10*	72	1.4×10^{14}	2.3×10^{10}
	40**	76	1.8×10^{14}	1.6×10^{10}
650	10*	---	---	1.7×10^{10}
	40**	---	---	2.0×10^{10}

* Taken at 1 micron from front surface, 0.8×10^{-3} dpa/s.

** Taken at 2.3 microns from front surface, 3.2×10^{-3} dpa/s.

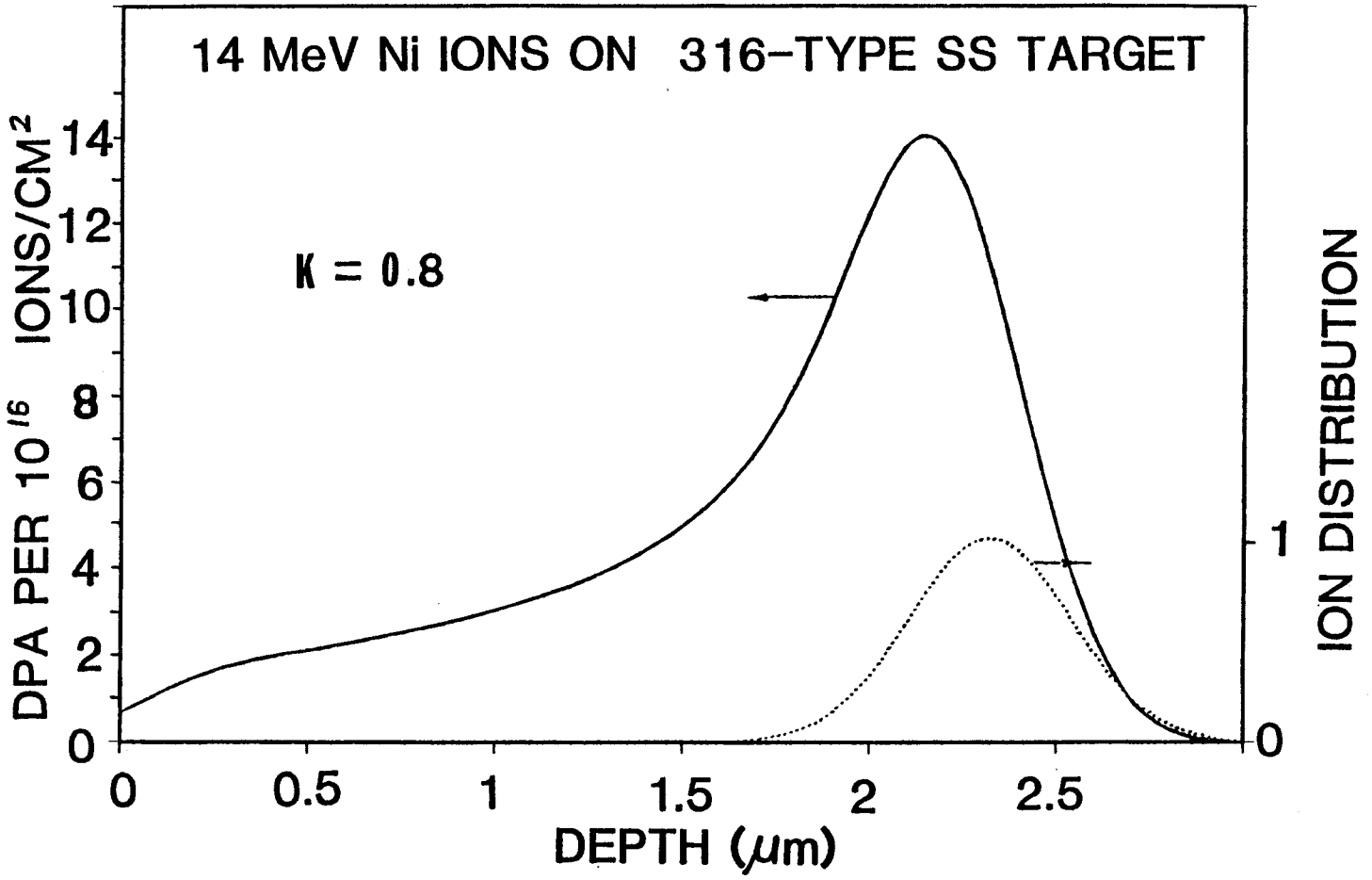

Fig. 1. Damage (dpa) vs. distance from the irradiated surface calculated using the Brice code [27]. The damage efficiency (K) used is 0.8. E_d = 40 eV.

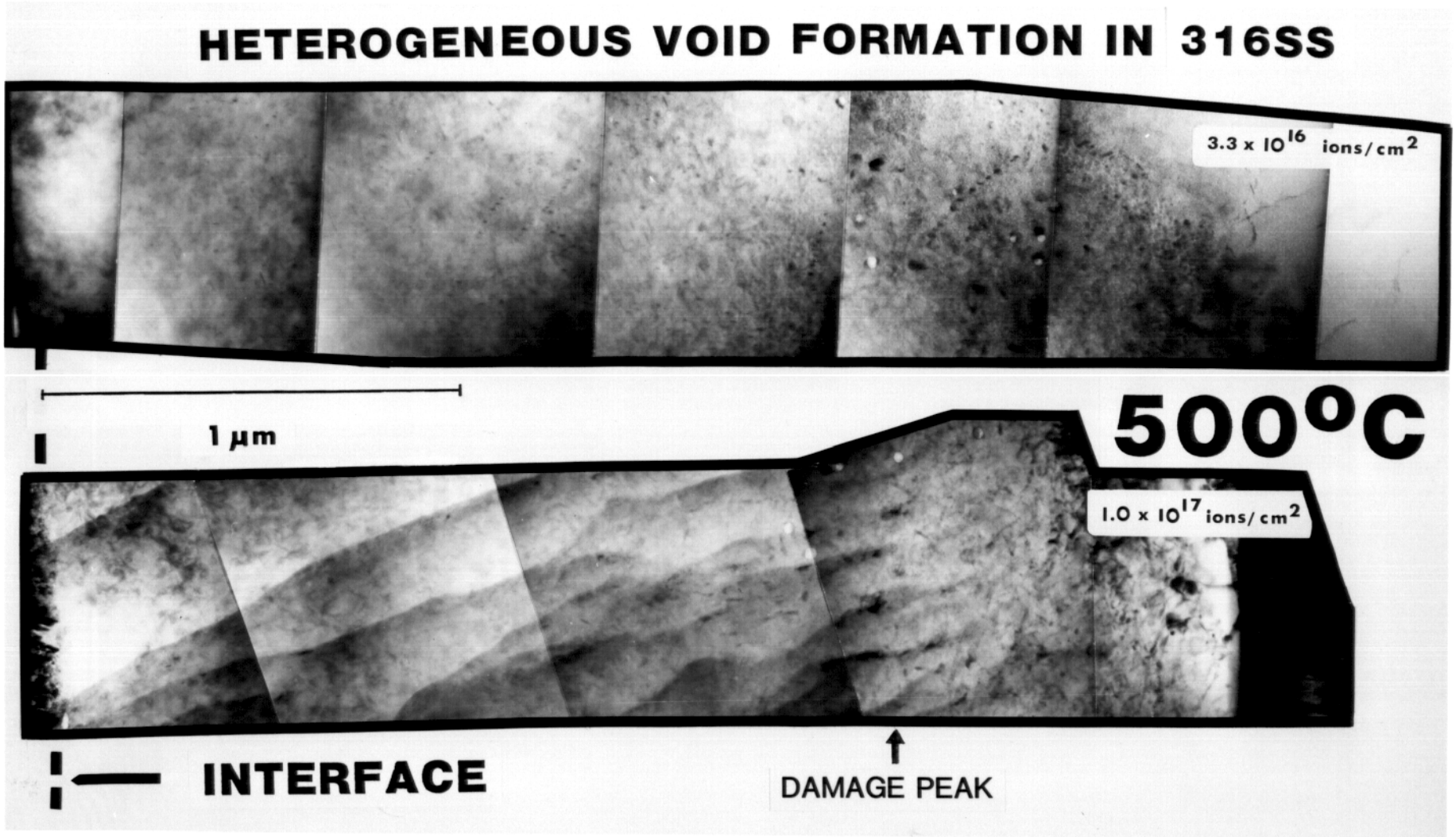

Fig. 2. TEM micrographs which span the entire damage region of 14 MeV Ni-ion irradiated 316 SS. Note the heterogeneous void formation.

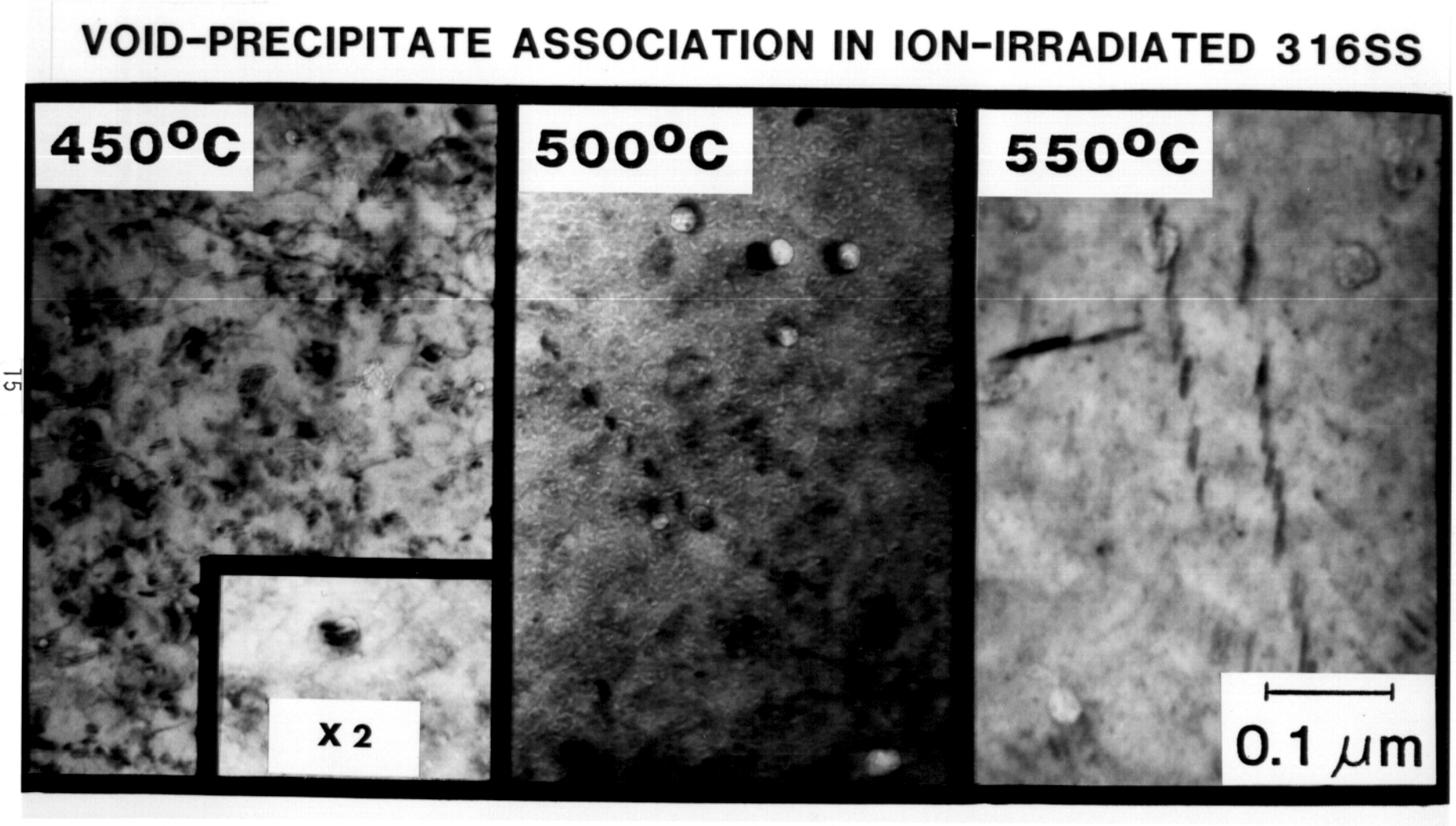

Fig. 3. Void structure in 316 SS after 14 MeV Ni-ion irradiation to 40 dpa. Note the precipitate-void association.

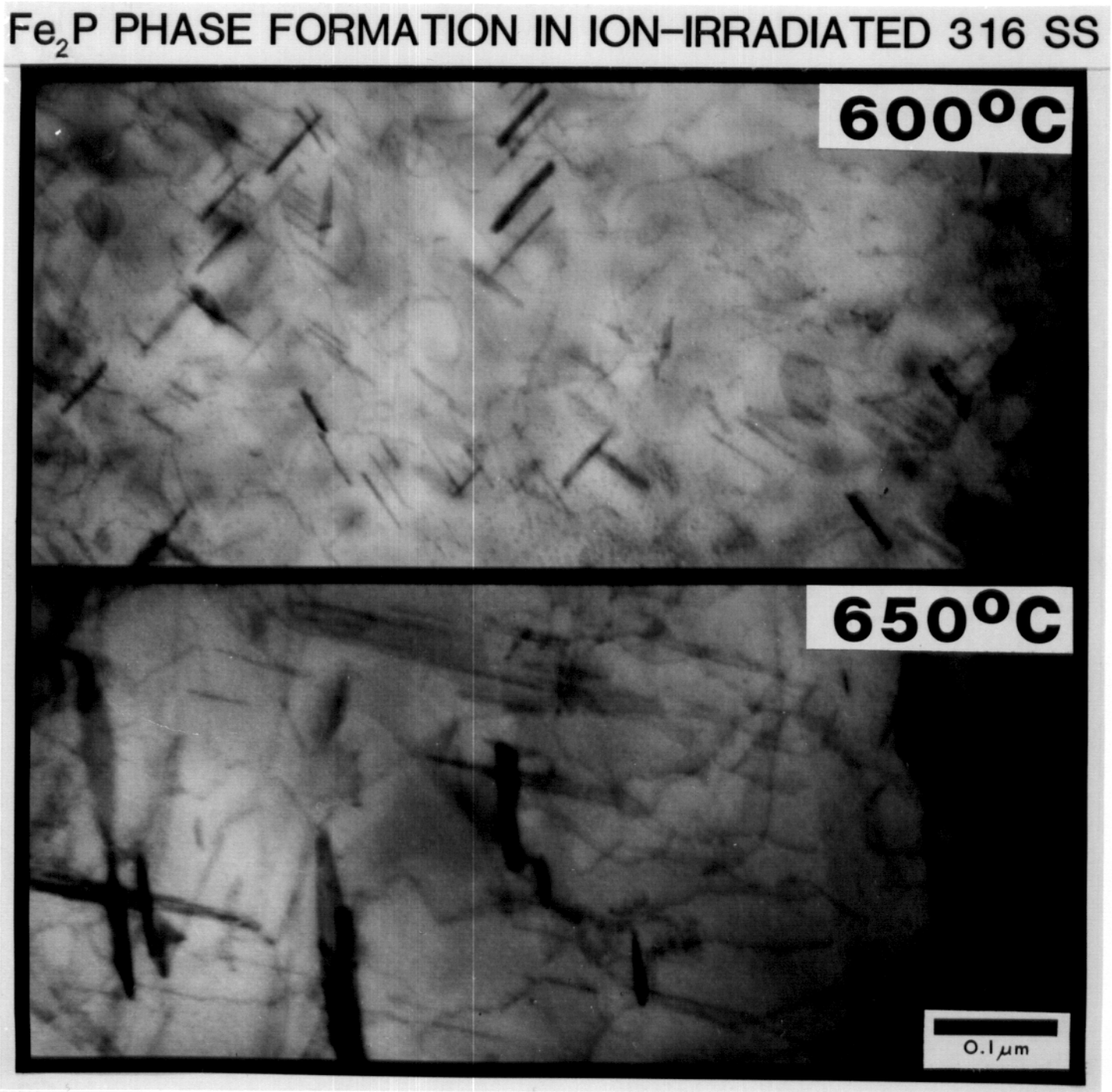

Fig. 4. Radiation-induced Fe_2P needles present in 316 SS after irradiation to 40 dpa. There were no voids detected at these irradiation conditions.

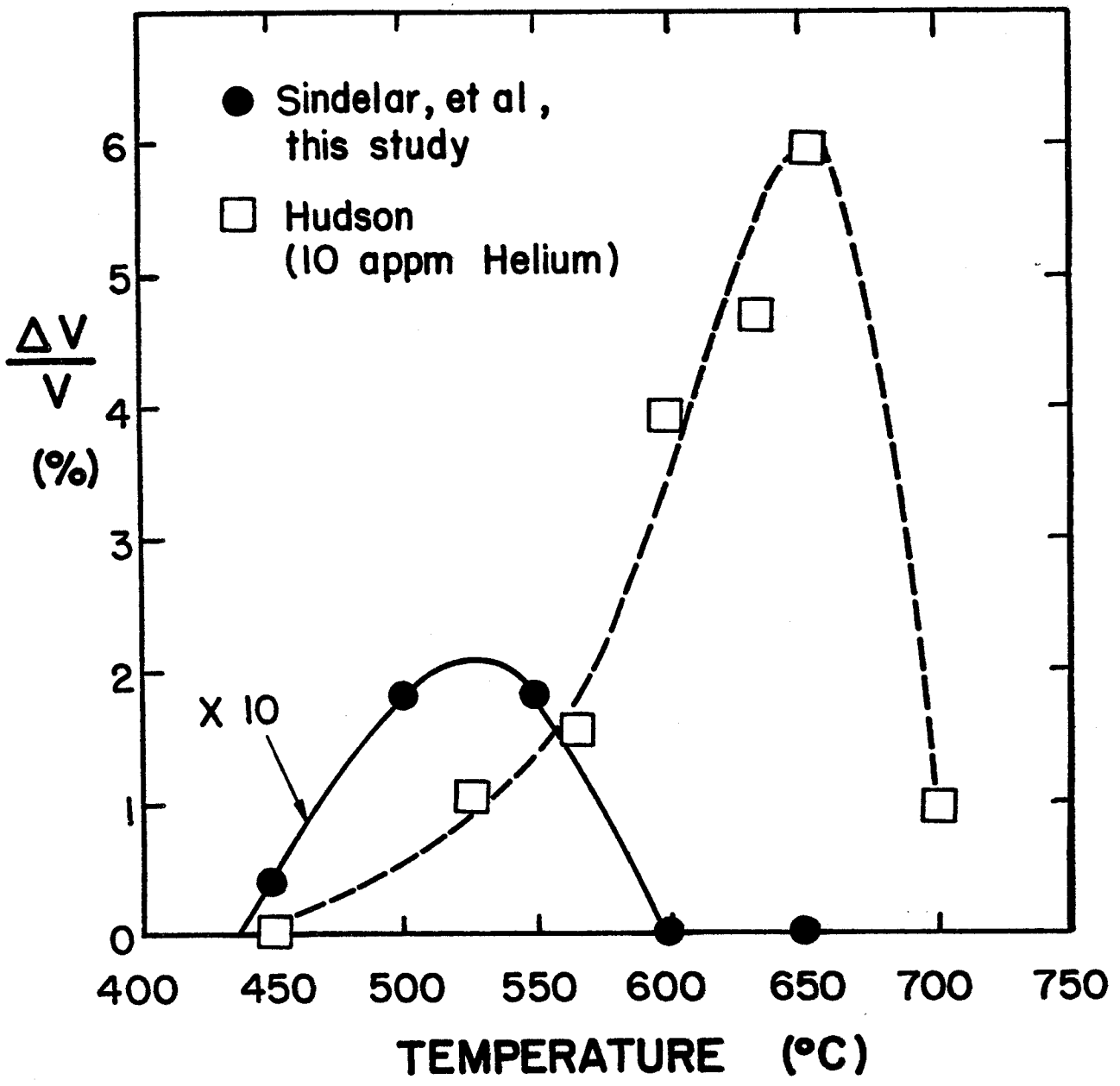

Fig. 5. Swelling curve for Ni-ion irradiated 316 SS to a common 40 dpa dose without gas (this study) and preinjected to 10 appm He (Hudson [11]).